Int. J. Heat Mass Transfer. Vol. 36, No. 7, pp. 1905–1912, 1993
Printed in Great Britain

0017–9310/93 $6.00+0.00

The effects of particle size distribution and refractive index on fly-ash radiative properties using a simplified approach

FENGSHAN LIU†
Department of Fuel and Energy, University of Leeds, Leeds LS2 9JT, U.K.

and

JIM SWITHENBANK
Department of Mechanical and Process Engineering, University of Sheffield, Sheffield S1 3JD, U.K.

(*Received* 28 *March* 1992)

Abstract—The radiative properties of a fly-ash polydispersion are calculated using a simplified approach based on Mie theory. The experimental data of fly-ash complex refractive index of Goodwin (Infrared optical constants of coal slags, Technical Report T-255, Stanford University, California) are employed in the calculation to take into account the wavelength-dependence of optical constants. The uncertainty in representing the particle size distribution is addressed explicitly. Due to this uncertainty, the uncertainty of the wavelength-integrated Planck mean absorption and scattering coefficients can be over 10%. The use of wavelength-independent optical constants for fly-ash yields unacceptable results of Planck mean coefficients.

1. INTRODUCTION

IN ORDER to predict radiative heat transfer in pulverized coal-fired systems, it is essential to know the radiative properties of combustion products. Indeed, it has been pointed out that accurate knowledge of the radiative properties of combustion products can be as important as the solution method [1]. Except radiation by water vapour and carbon dioxide, the particles present in a coal-fired furnace, including soot, coal, char and fly-ash, absorb and emit radiation in a continuous form covering the entire spectrum. It is believed that the major contributors to the continuum radiation are the fly-ash particles because char and soot particles are usually present in a relatively small fraction of the entire furnace volume and therefore they are not important in evaluating the overall heat transfer performance; however, fly-ash particles exist in almost the entire furnace volume [2].

In recent years, due to the important role played by fly-ash in radiative heat transfer in coal-fired furnaces, considerable attention has been paid to predicting their radiative properties and their effects on radiative heat transfer [3–7]. These studies have indicated that neglect of the ash radiation may underestimate total heat transfer by up to 30%. It should be noted that the predicted effects of fly-ash particles on radiation depend strongly on the absorption and scattering coefficients used in the calculations. These coefficients are in turn dependent on the complex index of refraction of ash, ash loading and ash particle size distribution.

Due to the lack of reliable and sufficient experimental data, most of the up to date studies have assumed that the optical constants n and k are independent of wavelength, with n taken in each case as 1.5 and k ranging from 0.005 to 0.05 [4–6, 8]. Only recently, Goodwin [9] has presented some more complete optical constants for homogeneous bulk samples with compositions similar to those of fly-ash. In the wavelength range from 0.5 to 12 μm which is of interest at furnace temperatures, their results indicate that the real part n does not exhibit strong wavelength-dependence; whilst the imaginary part k varies by several orders of magnitude.

By assuming fly-ash particles are homogeneous and spherical, the radiative properties of a single particle can be obtained from Mie theory [10]. However, the application of Mie theory is neither simple nor practical for engineering calculations. Fortunately, a simplified approach derived by van de Hulst [10] can be readily used to calculate the radiative properties of fly-ash particles as suggested by Menguc and Viskanta [6]. Almost without exception, it is assumed that each particle in the furnace scatters and absorbs radiation unaffected by the presence of other particles. Then the absorption and scattering of radiation by the particle suspension is calculated by a simple algebraic addition of the radiation absorbed and scattered by each particle. By expressing the size distribution of a fly-ash polydispersion as a three-parameter skewed distribution function [11], Menguc and Viskanta [6] were able to obtain a simple closed form solution for the spectral extinction and absorption coefficients using

† Present address: Department of Chemical Engineering, Queen's University, Kingston, Ontario, Canada K7L 3N6.

NOMENCLATURE

a, b	parameters in particle size distribution function
D	particle diameter [μm]
D_{10}	size-weighted diameter [μm]
D_{20}	r.m.s. diameter [μm]
I_b	black-body radiation intensity [W m^{-2} sr^{-1}]
k	imaginary part of refractive index
m	complex refractive index, $n-ik$
M	total number of particles analysed
M_i	differential number of particles
n	real part of refractive index
N	particle number density [m^{-3}]
Q_a	absorption efficiency factor
Q_e	extinction efficiency factor
Q_s	scattering efficiency factor
T	temperature [K]
x	particle size parameter.

Greek symbols

α	parameter in particle size distribution function
κ_a	absorption coefficient [m^{-1}]
κ_e	extinction coefficient [m^{-1}]
κ_s	scattering coefficient [m^{-1}]
λ	wavelength [μm].

Subscript

λ	spectral quantities.

Superscript

*	mean single particle properties.

the simplified approach. However, one of the three parameters in the particle size distribution function was assigned arbitrarily in the work of Menguc and Viskanta [6].

In this paper, the effect of the undetermined parameter in the particle size distribution on the fly-ash radiative properties is studied using the simplified approach. The wavelength-dependence of fly-ash optical constants is taken into account by employing the experimental data of Goodwin [9]. Numerical results show that the undetermined parameter can cause more than 10% uncertainty in the Planck mean absorption and scattering coefficients. A new condition is suggested to determine the arbitrary constant in the particle size distribution function used by Menguc and Viskanta [6]. This work also demonstrates that the Planck mean coefficients calculated using the wavelength-dependent optical constants differ significantly from those using wavelength-independent optical constants.

2. FLY-ASH MODEL

2.1. *Optical constants*

The optical constants of fly-ash presented by Goodwin [9] (see also Fig. 1(b) in ref. [7]) are employed in the present calculations. For the purpose of computer modelling, their experimental data of fly-ash optical constant are approximated by piecewise linear functions of wavelength. The real part n is written as

$$n = 1.5 \qquad 0.5 < \lambda < 6.0\ \mu\text{m}$$
$$n = 1.5-0.35(\lambda-6.0) \qquad 6.0 < \lambda < 8.0\ \mu\text{m}$$
$$n = 0.8+0.5(\lambda-8.0) \qquad 8.0 < \lambda < 11.0\ \mu\text{m}$$
$$n = 2.3-0.5(\lambda-11.0) \qquad 11.0 < \lambda < 12.0\ \mu\text{m}.$$

The imaginary part k is given as

$$k = 10^{-4.6+2.2(\lambda-0.5)} \qquad 0.5 < \lambda < 1.0\ \mu\text{m}$$
$$k = 10^{-3.5} \qquad 1.0 < \lambda < 4.0\ \mu\text{m}$$
$$k = 10^{-3.5+(\lambda-4.0)} \qquad 4.0 < \lambda < 5.0\ \mu\text{m}$$
$$k = 10^{-2.5+0.24(\lambda-5.0)} \qquad 5.0 < \lambda < 7.5\ \mu\text{m}$$
$$k = 10^{-1.9+1.8(\lambda-7.5)} \qquad 7.5 < \lambda < 8.5\ \mu\text{m}$$
$$k = 10^{-0.1} \qquad 8.5 < \lambda < 10.5\ \mu\text{m}$$
$$k = 10^{-0.1-0.733(\lambda-10.5)} \qquad 10.5 < \lambda < 12.0\ \mu\text{m}.$$

2.2. *Particle size distribution*

The fly-ash particles collected from a small-scale pulverized coal-fired furnace [12] are considered in this work. The particle size distribution, analysed by a Coulter counter, is summarized in Table 1. In this table, $f(D)$ is defined

$$f(D) = \frac{M_i}{M\Delta D_i} \times 100 \qquad (1)$$

where M is the total number of particles analysed. The mean fly-ash particle diameters D_{10} and D_{20} are calculated as

Table 1. Ash particle size distribution

D_i (μm)	Cumulative volume (%)	Differential No., M_i	ΔD_i (μm)	$f(D_i)$ (%)
4	100	63087	4.52	6.98
5.04	98.3	44035	1.175	18.74
6.35	94.8	32778	1.48	11.07
8.00	90.0	23975	1.875	6.39
10.1	83.3	16081	2.35	3.42
12.7	72.6	9498	2.95	1.61
16.0	60.6	5155	3.75	0.69
20.2	48.5	3045	4.7	0.32
25.4	34.3	1577	5.9	0.13
32.0	19.5	629	7.45	0.04
40.3	8.2	110	9.4	0.0
50.8	4.0	21	11.84	0.0
64.0	2.4	6	14.9	0.0
80.6	0.0	3	—	—

Table 2. Parameters of particle size distribution

α	a	b
2	0.04293	0.44118
3	0.01996	0.58824
4	0.00896	0.73529
5	0.00393	0.88235

$$D_{10} = \frac{\Sigma f(D_i) D_i \Delta D_i}{\Sigma f(D_i) \Delta D_i} = 6.80\ \mu\text{m} \tag{2}$$

$$D_{20} = \left(\frac{\Sigma f(D_i) D_i^2 \Delta D_i}{\Sigma f(D_i) \Delta D_i} \right)^{1/2} = 7.85\ \mu\text{m}. \tag{3}$$

The particle size distribution given in Table 1 can be expressed in a more concise functional form by using a three-parameter skewed distribution function [6, 11]

$$f(D) = aD^{\alpha} \exp(-bD). \tag{4}$$

In the work of Menguc and Viskanta [6], α was treated as a positive integer and its value was assigned arbitrarily; whilst the constants a and b were calculated from overall mean diameter D_{10} and the normalization of $f(D)$, i.e. the constants a and b obey the following relations:

$$\frac{a\alpha!}{b^{\alpha+1}} = 1 \tag{5}$$

$$\frac{a(\alpha+1)!}{b^{\alpha+2}} = D_{10}. \tag{6}$$

The values of a and b can be determined only if the value of α is assigned. For $\alpha = 2$, 3, 4 and 5, the corresponding values of a and b are given in Table 2. The effect of α on the particle size distribution is shown in Fig. 1. The size distribution function $f(D)$ is sensitive to the value of α. The larger the value of α, the larger the maximum of $f(D)$ and the particle diameter at which the maximum occurs. A larger α, however, yields a smaller particle diameter at which the maximum of $D^2 f(D)$ occurs, see Fig. 1(b).

In the prediction of radiative properties of a polydispersion, the size-weighted mean diameter D_{10} and the area-weighted mean diameter D_{20} are two important parameters since the size of the particles characterizes single particle properties and the area of the particles is required in evaluating the polydispersion properties. In this work, the following additional condition is suggested to determine uniquely the value of α

$$\frac{a(\alpha+2)!}{b^{\alpha+3}} = D_{20}^2 \tag{7}$$

i.e. the mean diameter D_{20} of the size distribution function, equation (4), is assumed to be equal to the measured value. The values of b, α and a can be evaluated from equations (5) to (7) such that

$$b = \frac{D_{10}}{D_{20}^2 - D_{10}^2} \tag{8}$$

$$\alpha = \frac{D_{10}^2}{D_{20}^2 - D_{10}^2} - 1 \tag{9}$$

$$a = \frac{b^{\alpha+1}}{\alpha!}. \tag{10}$$

For the particle size distribution given in Table 1, it is found that

$$\alpha = 2.0158$$

$$a = 0.04356$$

$$b = 0.4433.$$

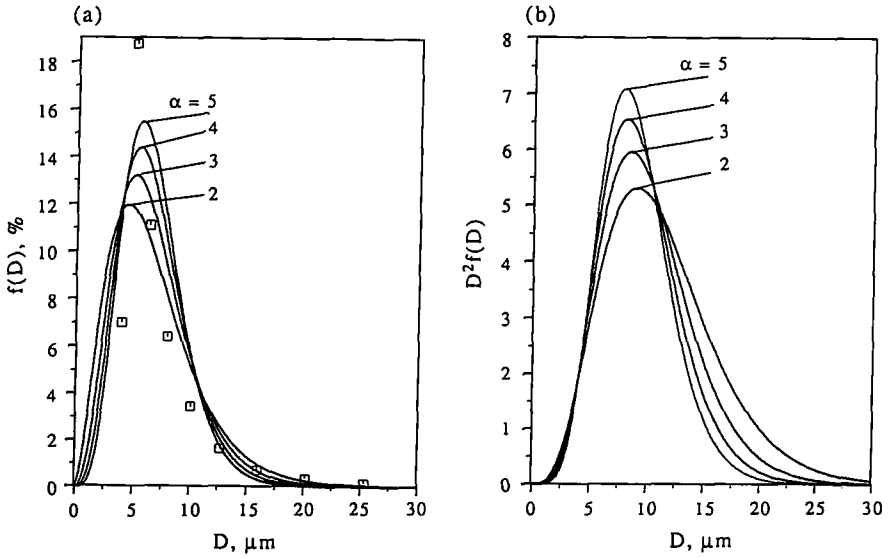

FIG. 1. Effect of α on the particle size distribution.

It is seen that this size distribution follows closely that with $\alpha = 2$ given in Table 2.

3. SPECTRAL RADIATIVE PROPERTIES

3.1. *Single particle characteristics*

Based on Mie theory, the radiative characteristics of a single particle is determined by the particle size parameter, $x = \pi D/\lambda$, and the complex refractive index, $m = n - ik$.

As derived by van de Hulst (Sections 11.22 and 11.23 in ref. [10]), the extinction and absorption efficiency factors can be calculated as

$$Q_e = 2 - 4\exp(-\rho\tan\beta)\frac{\cos\beta}{\rho}\sin(\rho-\beta) - 4\exp(-\rho\tan\beta)\left(\frac{\cos\beta}{\rho}\right)^2\cos(\rho-2\beta) + 4\left(\frac{\cos\beta}{\rho}\right)^2\cos 2\beta \quad (11)$$

$$Q_a = 2K(4xk) \quad (12)$$

where

$$\tan\beta = \frac{k}{n-1}, \quad \rho = 2x(n-1), \quad x = \frac{\pi D}{\lambda}$$

$$K(z) = \tfrac{1}{2} + \frac{e^{-z}}{z} + \frac{e^{-z}-1}{z^2}. \quad (13)$$

The scattering efficiency factor Q_s is then calculated by subtracting Q_a from Q_e. Essentially, these equations are applicable over the entire domain of the Mie theory if the real part of the refractive index n is close to 1.0 and even for values of n as large as 2.0 and the imaginary part k negligibly small.

It is clear that the complex refractive index of fly-ash presented by Goodwin [9] meets the conditions required by the simplified expressions for extinction and absorption efficiency factors except for the imaginary part k in the wavelength range $8.0 < \lambda < 11.0\ \mu m$.

The absorption and scattering extinction efficiency factors for a particle having diameter $D = D_{10}$ are shown in Figs. 2 and 3, respectively. The features seen in the absorption efficiency spectrum are similar to those in the spectrum of the imaginary part of the refractive index (see Fig. 1(b) in ref. [7]).

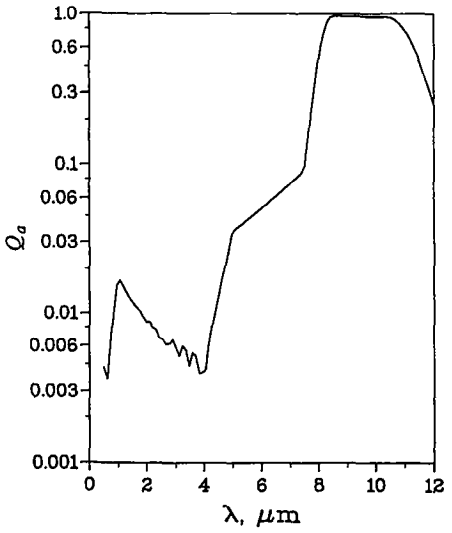

FIG. 2. Absorption efficiency factor Q_a. $D = D_{10}$.

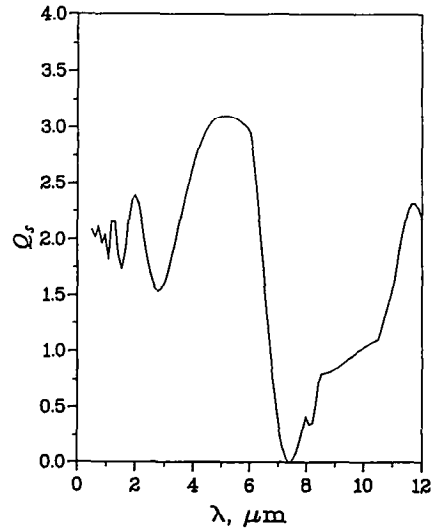

FIG. 3. Scattering efficiency factor Q_s. $D = D_{10}$.

3.2. *Spectral coefficients of the fly-ash polydispersion*

The spectral absorption, scattering and extinction coefficients of a cloud of fly-ash particles can be evaluated from

$$\beta_\lambda(m,N) = \int_0^\infty Q_\beta(D,\lambda,m)\frac{\pi D^2}{4}f(D)N\,dD \quad (14)$$

where β_λ stands for either spectral absorption coefficient $\kappa_{a\lambda}$, spectral scattering coefficient $\kappa_{s\lambda}$, or spectral extinction coefficient $\kappa_{e\lambda}$. Q_β is the corresponding efficiency factor, N the particle number density and $f(D)$ the normalized particle size distribution function given in equation (4).

Dividing equation (14) by N, the following expressions are obtained:

$$\kappa^*_{e\lambda} = \frac{\kappa_{e\lambda}}{N} = \int_0^\infty Q_e(D,\lambda,m)\frac{\pi D^2}{4}f(D)\,dD \quad (15)$$

$$\kappa^*_{a\lambda} = \frac{\kappa_{a\lambda}}{N} = \int_0^\infty Q_a(D,\lambda,m)\frac{\pi D^2}{4}f(D)\,dD. \quad (16)$$

Substitution of equations (4), (11) and (12) into equations (15) and (16) yields the closed form expressions for $\kappa^*_{e\lambda}$ and $\kappa^*_{a\lambda}$ after some mathematical manipulations

$$\kappa^*_{e\lambda} = \frac{\pi a}{4}(2J_1 - 4\cos\beta J_2 - 4\cos^2\beta J_3 + 4\cos^2\beta\cos 2\beta J_4) \quad (17)$$

$$\kappa^*_{a\lambda} = \frac{\pi a}{4}(J_1 + 2CJ_5 + 2C^2J_6) \quad (18)$$

where

$$J_1 = \frac{1}{b^{\alpha+3}}\Gamma(\alpha+3) \quad (19)$$

$$J_2 = \frac{\sin\left[(2+\alpha)\arctan\frac{A}{B} - \beta\right]}{A(A^2+B^2)^{1/2(\alpha+2)}}\Gamma(\alpha+2) \quad (20)$$

$$J_3 = \frac{\cos\left[(\alpha+1)\arctan\frac{A}{B} - 2\beta\right]}{A^2(A^2+B^2)^{1/2(\alpha+1)}}\Gamma(\alpha+1) \quad (21)$$

$$J_4 = \frac{1}{A^2 b^{\alpha+1}}\Gamma(\alpha+1) \quad (22)$$

$$J_5 = \frac{1}{\left(b+\frac{1}{C}\right)^{2+\alpha}}\Gamma(\alpha+2) \quad (23)$$

$$J_6 = \left(\frac{1}{\left(b+\frac{1}{C}\right)^{\alpha+1}} - \frac{1}{b^{\alpha+1}}\right)\Gamma(\alpha+1) \quad (24)$$

$$A = \frac{2\pi(n-1)}{\lambda}, \quad B = b + \frac{2\pi k}{\lambda}, \quad C = \frac{\lambda}{4\pi k}. \quad (25)$$

Results of spectral absorption, scattering and extinction coefficients for the fly-ash polydispersion are given in Figs. 4–6, respectively, for different values of α. It can be seen that the fine ripple structure exhibited by the Lorenz–Mie solutions at short wavelength ($\lambda < 2.5$ μm) for a single particle of diameter D_{10}, see Fig. 3, is cancelled out by integrating over the particle size distribution. The fly-ash particles are weakly absorbing at $\lambda < 5$ μm and become strongly absorbing at longer wavelengths which reflect the spectral variation of the imaginary part k. For the particle size distribution considered in this work, the spectral scattering and extinction coefficients first increase gradually till reaching maxima at 6.3 μm, then decrease sharply to minima at 7.5 μm. At this wavelength, the scattering coefficient is nearly zero. Beyond 7.5 μm, the scattering and extinction coefficients differ significantly from each other since the absorption coefficient is large in this wavelength

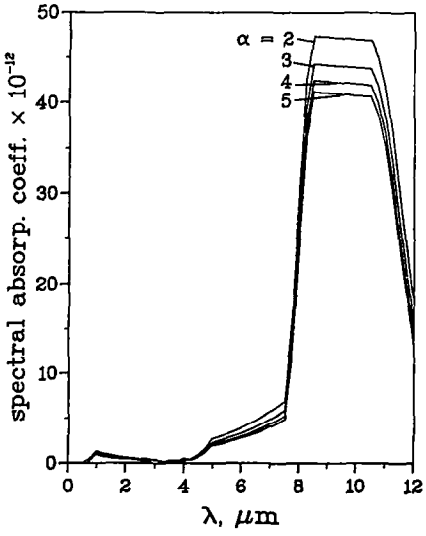

FIG. 4. Effect of α on the spectral absorption coefficient $\kappa^*_{a\lambda}$.

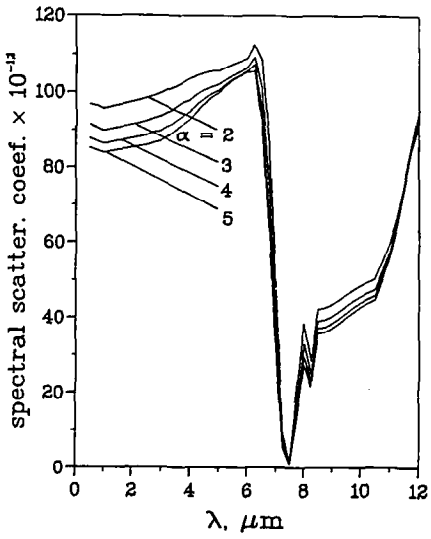

FIG. 5. Effect of α on the spectral scattering coefficient $\kappa^*_{s\lambda}$.

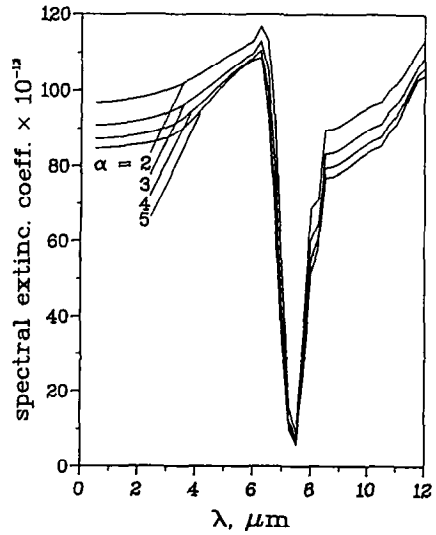

FIG. 6. Effect of α on the spectral extinction coefficient $\kappa^*_{e\lambda}$.

region. It should be noted that these features of the spectral absorption, scattering and extinction coefficients are similar to those presented by Goodwin and Mitchner [7] based on Mie calculations.

The effect of α on the spectral absorption coefficient is negligible at short wavelengths, $\lambda < 5$ μm, and becomes significant at longer wavelengths, see Fig. 4. While the effect of α on the scattering and extinction coefficients is considerable at wavelengths $\lambda < 6$ μm, see Figs. 5 and 6. At long wavelengths, $\lambda > 8.5$ μm, the extinction coefficient becomes sensitive again to the value of α. The smaller the value of α, the larger the spectral absorption, scattering and extinction coefficient due to the stronger weighting of large particle diameters, where $D^2 f(D)$ is high (see Fig. 1(b)).

4. PLANCK MEAN PROPERTIES

For most of the engineering calculations, the wavelength-integrated absorption and scattering coefficients are required since it is not always possible to perform radiative heat transfer calculations on a spectral level. The Planck mean coefficients defined below are of interest when the medium under consideration is optically thin

$$\kappa_a^* = \frac{\int_0^\infty \kappa_{a\lambda}^* I_{b\lambda}(T)\, d\lambda}{\int_0^\infty I_{b\lambda}\, d\lambda} \tag{26}$$

$$\kappa_s^* = \frac{\int_0^\infty \kappa_{s\lambda}^* I_{b\lambda}(T)\, d\lambda}{\int_0^\infty I_{b\lambda}\, d\lambda} \tag{27}$$

where $I_{b\lambda}(T)$ is the Planck spectral black-body intensity. These integrations can be performed numerically by dividing the entire wavelength spectrum into a number of bands such that

$$\kappa_a^* = \sum_{i=1}^{n} \kappa_{a\lambda}^* I_{b\lambda,i}(T)\Delta\lambda_i \Big/ \sum_{i=1}^{n} I_{b\lambda,i}(T)\Delta\lambda_i \tag{28}$$

$$\kappa_s^* = \sum_{i=1}^{n} \kappa_{s\lambda}^* I_{b\lambda,i}(T)\Delta\lambda_i \Big/ \sum_{i=1}^{n} I_{b\lambda,i}(T)\Delta\lambda_i. \tag{29}$$

The wavelength summations in equations (28) and (29) are performed numerically for the wavelength range from 0.5 to 12.0 μm. The fraction of the total black-body flux contained in this range is 0.971 at 1200 K and 0.990 at 1800 K with the excluded fraction primarily on the long wavelength side.

Numerical results of the Planck mean absorption and scattering coefficients obtained by using different values of α are shown in Figs. 7 and 8, respectively. The Planck mean absorption coefficient decreases with increasing temperature due to the stronger weighting of short wavelengths where the spectral absorption coefficient is low (see Fig. 4). The Planck

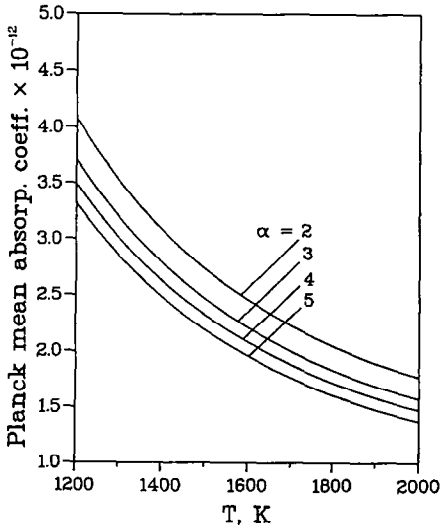

FIG. 7. Effect of α on the Planck mean absorption coefficient κ_a^*.

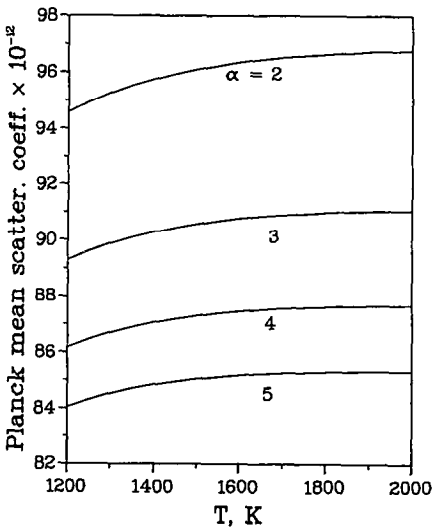

FIG. 8. Effect of α on the Planck mean scattering coefficient κ_s^*.

mean scattering coefficient increases with increasing temperature and is less temperature-dependent than the Planck mean absorption coefficient. It is worth noting that the variation trend of the Planck mean absorption coefficient with temperature is opposite to that presented by Viskanta *et al.* [4] using wavelength-independent optical constants; however, it is in agreement with the results of mean single-particle total emissivity calculated by Goodwin and Mitchner [7].

The figures also show that both the absorption and the scattering coefficients are sensitive to the value of α. As expected from Figs. 4 and 5, the smaller the value of α, the larger the Planck mean absorption and scattering coefficients. By varying the value of α from

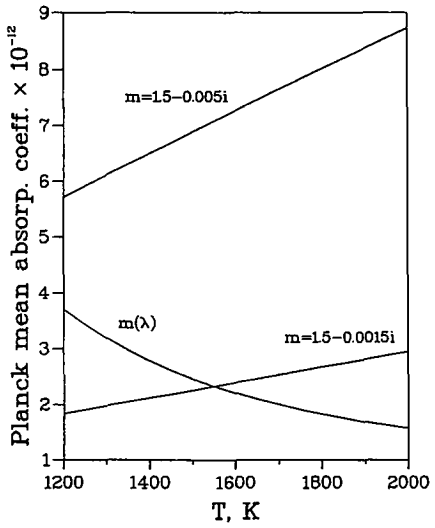

FIG. 9. Comparison of the Planck mean absorption coefficient κ_a^* based on wavelength-independent indices with that based on wavelength-dependent data.

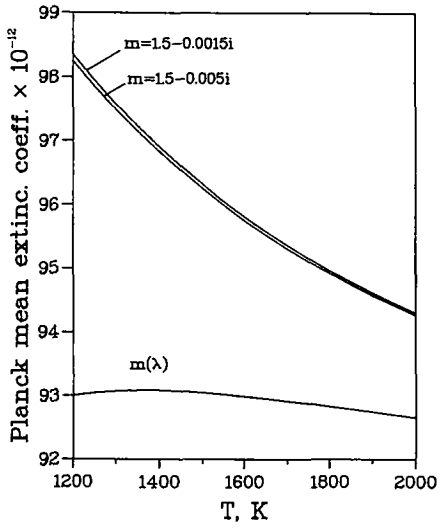

FIG. 11. Comparison of the Planck mean extinction coefficient κ_e^* based on wavelength-independent indices with that based on wavelength-dependent data.

2 to 5, there is more than a 10% decrease in both the Planck mean absorption and scattering coefficients.

Calculations have also been performed for wavelength-independent optical constants of $m_1 = 1.5 - i0.005$ and $m_2 = 1.5 - i0.0015$. The results are compared with those obtained using spectral optical constants in Figs. 9–11. The particle size distribution with $\alpha = 3$ (see Table 2) is used in these calculations. Figure 9 shows that the use of $k = 0.005$ overestimates the Planck mean absorption coefficient, while the use of $k = 0.0015$ yields a much closer result to that based on wavelength-dependent optical constants, except that they give different variation trends with temperature.

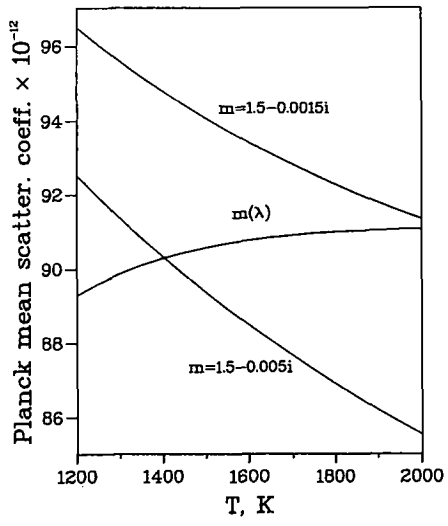

FIG. 10. Comparison of the Planck mean scattering coefficient κ_s^* based on wavelength-independent indices with that based on wavelength-dependent data.

In opposition to the effect of k on the mean absorption coefficient, the lower imaginary part k results in higher mean scattering coefficient, see Fig. 10. The smaller k (0.0015) overpredicts the mean scattering coefficient especially at temperatures $T < 1600$ K, while the larger k (0.005) overestimates the mean scattering coefficient at $T < 1400$ K and then underpredicts the mean scattering coefficient at higher temperatures.

Figure 11 shows the Planck mean extinction coefficients. It can be seen that the extinction coefficient calculated using spectral optical constants is almost constant in the temperature range considered. The Planck mean extinction coefficient based on wavelength-independent optical constants decreases with increasing temperature. In addition, the mean extinction coefficient is very insensitive to the value of the imaginary part k due to the insensitivity of the extinction efficiency factor to the value of k [12].

The results shown in Figs. 9–11 indicate that it is not acceptable to ignore the wavelength-dependence of optical constants in the prediction of fly-ash radiative properties. The average value of the imaginary part of the fly-ash complex refractive index $k = 0.012$ estimated by Gupta and Wall [13] is definitely too high to calculate the fly-ash radiative properties.

5. CONCLUSIONS

A simplified approach based on Mie theory has been employed to calculate the radiative properties of a fly-ash polydispersion. The experimental data of Goodwin [9] were used in the calculations to take into account the wavelength-dependence of fly-ash optical

constants. A new condition is suggested to determine uniquely the value of α present in the particle size distribution based on the consideration of the important role played by the mean particle diameter D_{20} in evaluating the radiative properties of polydispersions.

Numerical results show that the simplified approach is able to produce the important features of those based on Mie calculations presented in ref. [7]. The effect of the value of α on the fly-ash radiative properties is studied. The results indicate that the arbitrariness of α can easily cause more than 10% uncertainty in the Planck mean absorption and scattering coefficients. Based on the work of Menguc and Viskanta [14, 15], such uncertainty in radiative properties can give rise to significant uncertainty in the prediction of radiative heat transfer. Therefore, it is of importance to establish a criterion to eliminate the uncertainty in the radiative properties of fly-ash particles due to their size distribution.

By comparing the results of using wavelength-independent optical constants with those using measured fly-ash optical constants, it can be concluded that it is not acceptable to ignore the wavelength-dependence of fly-ash refractive index. Moreover, the previous studies employing $n = 1.5$ and k ranged from 0.005 to 0.05, seem to overestimate the Planck mean absorption coefficient and to underestimate the Planck mean scattering coefficient of fly-ash particles.

REFERENCES

1. R. Viskanta and M. P. Menguc, Radiative heat transfer in combustion systems, *Prog. Energy Combust. Sci.* **13,** 97–160 (1987).
2. A. G. Blokh, *Heat Transfer in Steam Boiler Furnaces*, Chap. 3. Hemisphere, Washington, DC (1988).
3. T. F. Wall, A. Lowe, L. J. Wibberley, T. Mai-Viet and R. P. Gupta, Fly ash characteristics and radiative heat transfer in pulverised-coal-fired furnaces, *Combust. Sci. Technol.* **26,** 107–121 (1981).
4. R. Viskanta, A. Ungan and M. P. Menguc, Predictions of radiative properties of pulverised coal and fly-ash polydispersions, ASME paper 81-HT-24 (1981).
5. R. P. Gupta, T. F. Wall and J. S. Truelove, Radiative scatter by fly ash in pulverised-coal-fired furnaces: application of the Monte Carlo method to anisotropic scatter, *Int. J. Heat Mass Transfer* **26,** 1649–1660 (1983).
6. M. P. Menguc and R. Viskanta, On the radiative properties of polydispersions: a simplified approach, *Combust. Sci. Technol.* **44,** 143–159 (1985).
7. D. G. Goodwin and M. Mitchner, Flyash radiative properties and effects on radiative heat transfer in coal-fired systems, *Int. J. Heat Mass Transfer* **32,** 627–638 (1989).
8. S. A. Boothroyd and A. R. Jones, Radiative transfer scattering data relevant to fly ash, *J. Phys. D: Appl. Phys.* **17,** 1107–1114 (1984).
9. D. G. Goodwin, Infrared optical constants of coal slags, Technical Report T-255, Stanford University, California (1986).
10. H. C. van de Hulst, *Light Scattering by Small Particles*. Wiley, New York (1957).
11. C. L. Tien, D. G. Doornink and D. A. Rafferty, Attenuation of visible radiation by carbon smokes, *Combust. Sci. Technol.* **6,** 55–59 (1972).
12. F. Liu, New development in pulverized coal combustion: numerical modelling of radiative heat transfer and experimental test of a novel burner technique, Chap. 7, Ph.D. Thesis, University of Sheffield, U.K. (1990).
13. R. P. Gupta and T. F. Wall, The complex refractive index of particles, *J. Phys. D: Appl. Phys.* **14,** L95–98 (1981).
14. M. P. Menguc and R. Viskanta, A sensitivity analysis for radiative heat transfer in a pulverized coal-fired furnace, *Combust. Sci. Technol.* **51,** 51–74 (1987).
15. M. P. Menguc and R. Viskanta, Radiative transfer in axisymmetric, finite cylindrical enclosures, *J. Heat Transfer* **108,** 271–276 (1986).